International Journal of Mechanical, Industrial and Aerospace Sciences
ISSN: 2517-9950
Vol:7, No:3, 2013

# Design and Microfabrication of a High Throughput Thermal Cycling Platform with Various Annealing Temperatures

Sin J. Chen and Jyh J. Chen

***Abstract*—**This study describes a micro device integrated with multi-chamber for polymerase chain reaction (PCR) with different annealing temperatures. The device consists of the reaction polydimethylsiloxane (PDMS) chip, a cover glass chip, and is equipped with cartridge heaters, fans, and thermocouples for temperature control. In this prototype, commercial software is utilized to determine the geometric and operational parameters those are responsible for creating the denaturation, annealing, and extension temperatures within the chip. Two cartridge heaters are placed at two sides of the chip and maintained at two different temperatures to achieve a thermal gradient on the chip during the annealing step. The temperatures on the chip surface are measured via an infrared imager. Some thermocouples inserted into the reaction chambers are used to obtain the transient temperature profiles of the reaction chambers during several thermal cycles. The experimental temperatures compared to the simulated results show a similar trend. This work should be interesting to persons involved in the high-temperature based reactions and genomics or cell analysis.

***Keywords*—**Polymerase chain reaction, thermal cycles, temperature gradient, micro-fabrication.

## I. Introduction

IN the past decades, there has been an increased demand for rapid and accurate detection of bacteria, viruses, and protozoa. The control of microbiological hazards to reduce the incidence of infectious diseases requires simultaneous detection of multiple microbial pathogens. Traditional cell culture methods are time consuming, and some pathogens are not cultivable. With recent advances in polymerase chain reaction (PCR) method [1], a rapid method for quantization of the pathogen load has been realized. And PCR has become one of the most popular and widely used DNA amplification techniques in molecular biology, forensic analysis, and medical diagnostics. The methods of disease diagnosis have been moving from conventional cell-culture processes to molecular level detection.

PCR was first performed in multiple water baths, and then in programmable heat blocks or thermal cyclers. A specific DNA sequence is amplified by an enzymatic reaction using repetitive cycling between three temperatures. Each thermal cycle includes 90-95 °C for denaturation, 50-70 °C for annealing, and 70-75 °C for extension. Due to a large thermal mass and associated slow heating and cooling rates, PCR might take as long as 2 hours with the conventional devices. With the advancement in the microelectromechanical system (MEMS) technology, miniaturized PCR devices have been developed. Northrup et al. [2] presented a silicon based PCR chip. The battery-operated system showed significant improvements over the commercial thermal cycling instrument. Since then, many types of PCR chips have been introduced. Various types of microreactors, including microchambers, microchannels, and droplets, were employed for miniature DNA amplifications. These microreactors utilized the reduced assay time, the portability, as well as the low sample consumption.

In the past, multiplex PCR was reported as a high throughput platform for simultaneous analyses of multiple gene targets. Xiang et al. [3] presented a miniature PCR device consisting of a multi-reactor chip and a thermal cycler. The cycler consisted of a thin film heating element and a fan for rapid cooling. Real-time PCR of *E. coli* stx1 had been demonstrated with the device. Ohashi et al. [4] described a multiple droplet-based PCR device using magnetic transportation system. The droplet-based oscillatory thermal cycling was performed by moving the droplets to the designated temperature zones on the flat plate. The five PCR products ranging from 126 to 1219-bp were successfully provided in this device. Sun et al. [5] reported a multichannel closed-loop magnetically actuated microchip for PCR. The microchip was placed on top of three heating blocks. High reproducibility was achieved for different channels in the same run. Ramalingam et al. [6] reported a micro PCR chip comprising an array of reactors, pre-loaded with primer pairs for simultaneous PCR analyses of multiple waterborne pathogens. The temperature of the microchip was cycled using a thermoelectric cooler. This platform was able to detect and quantify water borne pathogens. Zhang and Xing [7] developed a strategy for executing parallel DNA amplification in the microfluidic gradient (MG) PCR device. A temperature gradient device was constructed by assembling together the fin array heat sink, a resistance cartridge heater, and a fan. The MG-PCR from three parallel reactions of 112-bp DNA fragment was performed. Wulff-Burchfield [8] evaluated a microfluidic real-time PCR platform. PCR reactions were run on the platform, consisting of 4 reactions each on 5 separate 4-loop chips. The real-time PCR was easier to use and nearly 3 times faster than the conventional real-time PCR. Sugumar et al.

S. J. Chen is with the Department of Biomechatronics Engineering, National Pingtung University of Science and Technology, Pingtung 91201, Taiwan (phone: 886-8-7723202 ext.7029; fax: 886-8-7740420; e-mail: e2458245990@yahoo.com.tw).

J. J. Chen is with the Department of Biomechatronics Engineering, National Pingtung University of Science and Technology, Pingtung 91201, Taiwan (corresponding author to provide phone: 886-8-7723202 ext.7029; fax: 886-8-7740420; e-mail: chaucer@mail.npust.edu.tw).

[9] used a rotary-linear motion PCR device to do the multiple sample DNA amplification. The sample chambers were rotated in a clockwise direction to shift from one temperature zone to next zone. It shows a result in successfully amplifying the 150-bp DNA samples. Liu et al. [10] presented the development of a capillary-based oscillation droplet approach of a continuous-flow PCR. The reaction plugs were pumped back and forth between two heating blocks using a multi-channel syringe pump. The capillary PCR assay accounted for only 20% of the amplification time needed in a conventional PCR.

In this paper we present a simple way of producing a temperature gradient polydimethylsiloxane (PDMS)-glass bonding PCR chip. The temperature of the chip is cycled. Two cartridge heaters are placed at two sides of the chip. They are maintained at the same temperature during the denaturation and the extension steps, and at two different temperatures to achieve a temperature gradient on the chip during the annealing step. In this prototype, commercial software is utilized to determine the chip materials and geometric parameters those are responsible for creating the denaturation, annealing and extension temperatures within the chip. A linear temperature gradient can be created in the chip during the annealing step. The measured temperatures compared to the simulated results are also shown.

## II. Theoretical Model and Numerical Method

### A. Theoretical Model

In this study, the PCR chip repeatedly cycled among three temperature processes. The chip absorbs the thermal energy from the heater and then the thermal energy is transmitted into the chip. And the chip also dissipates the thermal energy to the environment by ambient air. The heat transfer mechanisms contain thermal conduction and heat convection. The physical configuration is presented in Fig. 1 for modeling the heat transfer of the PCR chip which are exposed to the air convection and/or the isothermal heating. As no forced air flow is supplied, natural convection would be the mechanism that brings the thermal energy out of the chip surface. Heaters are assumed to be placed under the chip and contacted perfectly with the chip to maintain the designed temperature as required for PCR processes. The physical properties of the chip are kept unchanged during thermal cycles.

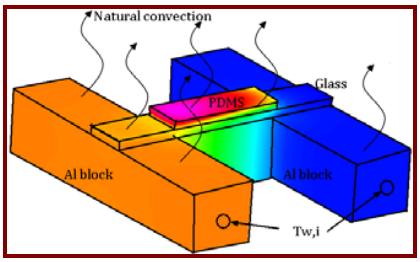


Fig. 1 The physical configuration of the chip

The governing equations for a three-dimensional transient energy transfer problem can be written as followings to predict the unsteady temperature of the chip.

$$\frac{\partial T}{\partial t} = \alpha \nabla^2 T \tag{1}$$

where T is the temperature. t is the time. α is the thermal diffusivity. The thermophysical properties are temperature-independent and uniform through the entire chip.

The initial and boundary conditions for energy equations are thus as follows. During the thermal cycling process, the entire system is assumed to be the same temperature, $T_0$, at the beginning.

at $$t = 0, T = T_0 \tag{2}$$

A pre-determined temperature is assumed at each of the heaters. The temperature is uniform along the heater surface. The glass wafer is coated by a thermal paste to be thermally connected to the aluminum blocks. The temperature zones in the device supported by the separate heaters supply a uniform temperature input, and the isothermal boundary condition is utilized.

$$T(t)_{Heater\ \ surface} = T_{w,i} \tag{3}$$

where $T_{w,i}$ is the denaturation, annealing, or extension temperature of the heater for i equals to 1, 2 or 3, respectively. The duration of each step during PCR is specified.

The convective boundary condition is used on all external surfaces except the heater surfaces.

$$-k\frac{\partial T}{\partial n} = h(T - T_\infty) \tag{4}$$

where k is the thermal conductivity of the chip material. h is the convective heat transfer coefficient between the outer surface and the ambient. $T_\infty$ is the ambient temperature. As a general rule, a nature convection boundary condition, with a coefficient of 6.5 W/m$^2$K [11], is assumed. The boundary conditions between each solid part of the entire system are a continuous temperature and heat flux.

### B. Numerical Method

Numerical simulation is carried out to investigate the thermal behavior of the PCR device. The device has been modeled to assess the thermal properties such as temperature distribution, transient temperature variation, heating, and cooling rates. For this modeling a 3D heat transport model has been used as well as finite volume modeling in CFD-ACE+$^{TM}$.

The computational domain is divided into a number of cells known as control volumes. The governing equations are numerically integrated over each of these computational cells or control volumes. A structured grid system with good

orthogonality is recommended for accurate prediction and reliability. In this study the geometric model for the three dimensional rectangular structure is considered. Therefore, the structured grid system is utilized directly. In the computation of the enthalpy of the simulation model, the spatial discretizations are performed using a second-order upwind scheme with limiter [12]. The conditions of convergence can be divided into two kinds. The first one is the maximum number of the solver iterations. The second one determines the convergence criteria to be used. In this study, we perform 500 sweep times and use $10^{-4}$ as the convergence criterion. Grid sensitivity is evaluated using different element sizes to ensure that the simulated results are independent of element size. A simple time step dependence study is useful to determine the effect of the time step size on the accuracy of the results. The process is repeated until the similarity in results is within the acceptable solution tolerance (0.1%). The time step is taken to be small and a Courant number of less than 1.0 is used [13]. At the initial time steps, approximately 100 sweep times are required to obtain convergent solutions at each time step, and the iterations are greatly reduced with lapse of time. The overall computational time for predicting the heat transfer in our system is about 2 hours per case at the personal computer with E8400 CPU and 2G RAM.

## III. Experimental Setup

The experimental setup, which involves a PCR chip, two heater modules, and two cooling fans, is prepared and shown in Fig. 2. For experimental characterization of temperature variation, the PCR chip with multi chambers are fabricated by soft lithography techniques. For the thermal visualization, an infrared (IR) camera is used to measure the temperature distribution in the PCR device. To verify the simulation results, the chamber temperatures are monitored using the thermocouples which are connected to a data acquisition system. Different operational parameters are considered to investigate the effects on the temperature distribution of the designed chip.

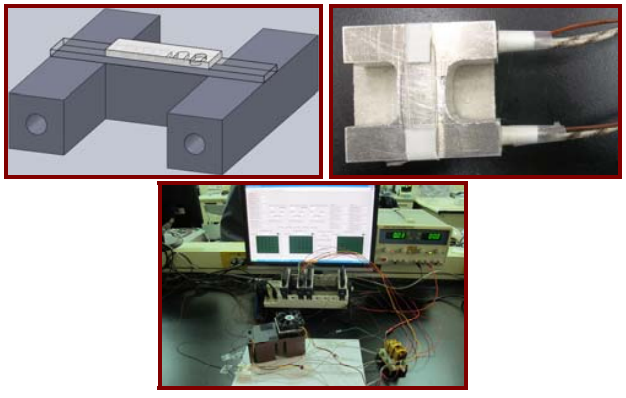

Fig. 2 The experimental setup of the designed system

A PDMS-glass bonding microfluidic chip is fabricated using the standard soft-lithography and PDMS casting techniques mentioned detailedly in [14]. Fig. 3 schematically shows the soft-lithography process. The layout of the PCR chambers is patterned on a transparent film, as an optical mask. Initially, a silicon wafer is cleaned and dehydrated on a hotplate. The microchannel is fabricated by spin-coating an SU-8 photoresist layer on a silicon substrate. The photoresist is then pre-baked and soft baked on a hotplate. After the UV exposure and the development, the wafer is hard baked. Once the mold is complete, the wafer is rinsed in deionized (DI) water and dried with nitrogen. Liquid Sylgard 184 pre-polymer and its curing agent are thoroughly mixed in a weight ratio of 10:1. The mixture is degassed to remove bubbles generated during the mixing and poured into a SU8 mold. The PDMS is cured at 75 °C subsequent to the degassing. After pouring the PDMS mixture onto the SU-8 patterned master, the PDMS is then cured in a convection oven and the replicas are peeled off carefully from the master. The solidified pattern is then removed and trimmed to the size of the glass substrate. Methanol is used as a surfactant to prevent the oxygen-plasma-treated PDMS replica and glass slide from being irreversibly bonded when aligned improperly. The prepared PDMS is then bonded to the glass slide after oxygen plasma treatment. The bonded chip is baked overnight.

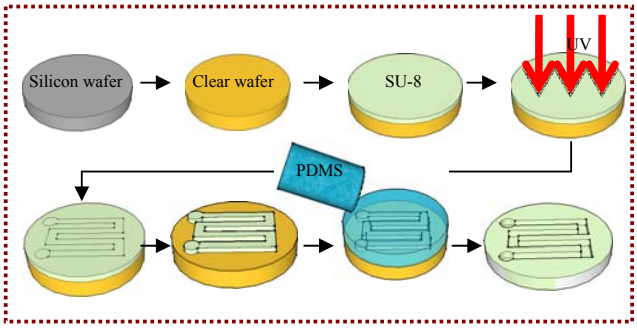


Fig. 3 Schematic diagram of the microfabrication process of SU-8 molds and the PDMS chip

The PDMS layer (1 mm thick) harboring microchambers is bonded to 1 mm thick glass substrate. Our chip consists of five microchambers with a width of 1.55 mm, a length of 3.55 mm, and a depth of 0.9 mm, which is about equivalent of 5 $mm^3$ of the reaction volume. The overall dimension of the PCR chip is 25 mm × 5 mm. The temperature of the chamber area is measured by using a temperature sensor. The mixture is injected into the chamber through the opening. Mineral oil is used to cover the access holes of the microchip to prevent evaporation of the PCR mixture. After a designated number of thermal cycles, such as 25-35 cycles, the reagent can be taken out of the chamber for further analysis.

The temperature of the chip is cycled using two cartridge heaters and fans. A thermocouple is mounted on the heater surface to measure the temperature and used as the feedback control. The chip is placed on two cartridge heaters. Two

cartridge heaters are maintained at the same temperature during the denaturation and extension steps, and at two different temperatures to achieve a temperature gradient on the chip during the annealing step.

Heating is provided with two aluminum blocks which are under the chip. The high thermal conductivity of aluminum ensures good temperature uniformity within each block. Each heat block is equipped with one bore (about 3.2 mm). The bore houses the resistance cartridge heater (3.175 mm diameter, 3.8 mm length, 14 W, C1J-9412, Watlow, USA), and a K-type thermocouple (K30-2-506, Watlow, USA). A small amount of thermal grease is applied between these contacting thermal elements to ensure uniform thermal contact. The temperature difference of the block surface at three measured points is about ±1 K. The thermal cycling is controlled with a LabVIEW$^{TM}$ (National Instruments, Austin, TX) program through a control module. The temperature acquired with the thermocouple is used as the feedback signal for the PID controller programmed in LabVIEW$^{TM}$. The controller applied constant (100%) power during the heating period. Three sets of PID gains corresponding to each step of a cycle are employed when the temperature approaches the prescribed, set temperatures. After the introduction of the sample, all two heaters are programmed to maintain 95 °C (368 K). Subsequently, the chip is heated to 368 K, the chip is maintained at a linear temperature distribution ranging from 50 °C (323 K) to 60 °C (333 K), and then the chip is maintained at 72 °C (345 K). The whole system is insulated. At the completion of the heating cycles, two heaters are set to 345 K to facilitate the final step. The other thermocouples which are used to sense the central temperature of the chambers and two heating blocks are connected to a data acquisition system (model NI 9211, National Instruments, USA) that converts the analog signal to a digital one. A computer receives the temperature signals through the NI 9211 interface and records the real-time temperature profiles.

An infrared (IR) camera is also used to measure the temperature distribution in the PCR device in order to evaluate the numerical results. The top of the PCR chip is sprayed with a thin layer of a black paint suitable for thermal investigations. An IR camera (TVS-100, AVIO, Japan) connected to a personal computer is used to monitor the surface temperature distribution of the PCR chip in real-time starting when power is supplied to the heaters. The system and camera are enclosed in a black box to shield the device from ambient optical and thermal disturbances. After a steady state temperature distribution is achieved, IR images of the PCR device are captured. The captured digital images are then converted into temperature profiles.

## IV. Results and Discussion

In the following section we show the heat transfer in the PCR device exposed to three isothermal heating steps. The initial temperatures of the PCR chip are 300 K, i.e., at the temperature of the environment. This study presents the effects of the geometric and operational parameters on the temperature distribution of the PCR chip. The denaturation temperature is set at 367 K, the annealing temperatures ranged from 323 K to 333 K, and the extension temperature at 345 K. Analysis is performed for the first one complete cycle. It is assumed that the analysis of the remaining cycles will be the same. The thermal properties of PDMS, glass, and aluminum used in the simulations are listed in Table I.

TABLE I
THE THERMAL PROPERTIES OF PDMS, GLASS, AND ALUMINUM USED IN THE NUMERICAL SIMULATIONS

| | Thermal conductivity (W/m K) | Density (kg/m$^3$) | Specific heat (J/kg K) |
|---|---|---|---|
| PDMS | 0.15 | 970 | 1460 |
| Glass | 0.78 | 2400 | 840 |
| Aluminum | 210 | 2698.9 | 900 |

The simulation result of the transient temperature profile under constant heating temperatures is illustrated in Fig. 4. A PCR cycle for the central temperature of the chamber in the middle of the chip is shown. The temperatures of the heaters are programmed to maintain at 369 K for 11 s, then 323 K and 333 K for 14 s, and 347 K for 15 s (dashed lines in Fig. 4). The total cycling time is 40 s. The 5 s, 7s, and 10 s heating durations are assumed for PCR steps of the denaturation, annealing, and extension, respectively. After reaching the denaturation step the ramping rate of the chamber temperature is slower than that of the heater temperature. Then the center temperature of the chamber is lower than the set heater temperature during the denaturation step. After going through the annealing step, some thermal energy inside the interior region of the chamber is dissipated to the exterior and the central temperature is higher than the ambient temperature. It is found that the annealing temperature of the chamber in the middle of the chip is between the heater temperatures of 323 K and 333K. Finally, the center temperature of the chamber is lower than the set heater temperature during the extension step. The result shows that the center temperature of the chamber can achieve the reaction temperature during the reaction process. All three temperature steps have sufficient heating duration to perform PCR.

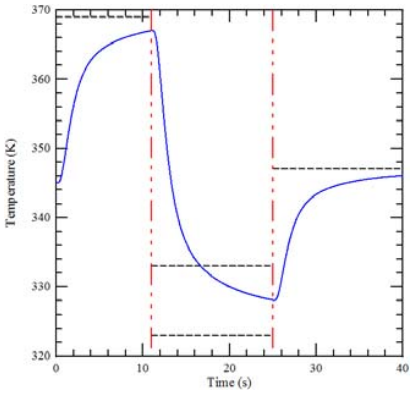


Fig. 4 The center temperature profile of the chamber

The results of the temperature profiles along the central line

of the chip on the cross section at the depth of 1 mm below the chip surface are expressed in Fig. 5. Fig. 5 shows the temperature gradients for the heating durations for one complete cycle at 11 s (denaturation), 25 s (annealing), and 40 s (extension). For a PDMS-glass bonding chip, the temperature at the cross-sectional area under 1 mm from the chip surface is almost constant at the denaturation and extension steps due to the high thermal conductivity of aluminum. Near the edge of the chip, temperature gradually increases (at the denaturation and extension steps) or decreases (at the annealing step) due to the lateral conduction and ambient convection effects. However, good temperature uniformity over 96.5% areas of the denaturation and extension steps is observed. For the annealing step, a linear temperature profile from 322 K to 332 K can be demonstrated. Among PCR amplifications, different kinds of DNA templates are often used, and therefore the annealing temperature should be optimized to reach an effective and specific DNA amplification. In our design, a PCR chip with different annealing temperatures for multichambers is reported. A linear annealing temperature profile is easily used to optimize the annealing temperature of a specific DNA.

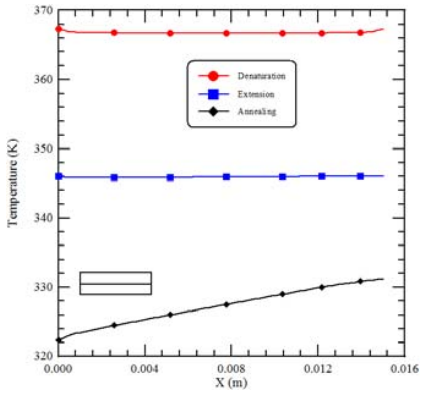


Fig. 5 The simulation results of the temperature profiles along the central line on the cross section at the depth of 1 mm below the chip surface

The estimated temperature distributions over the PCR chip on the cross section at the depth of 1 mm below the chip surface at 11 s (denaturation), 25 s (annealing), and 40 s (extension) are presented in Fig. 6. At the denaturation step, the temperature varies from 365.8 K to 367.4 K, shown in Fig. 6(a). At the extension step, we can find in Fig. 6(c) that the temperature ranges from 345.2 K to 346.2 K. Then it shows very good temperature uniformity. Without considering the PCR sample in the chambers, the device provide uniform temperature zone. The key component is the uniform temperature platform, the aluminum block, which is used under the chip. At the annealing step in Fig. 6(b), a smooth linear temperature distribution is illustrated. Furthermore, the temperatures along the Y direction are almost the same. In the measurement of the chambers' temperatures, some thermocouples are used to sense the central temperatures of the chambers. Thus the measured points located along the central line of the chip can be utilized to obtain the temperatures of the chambers.

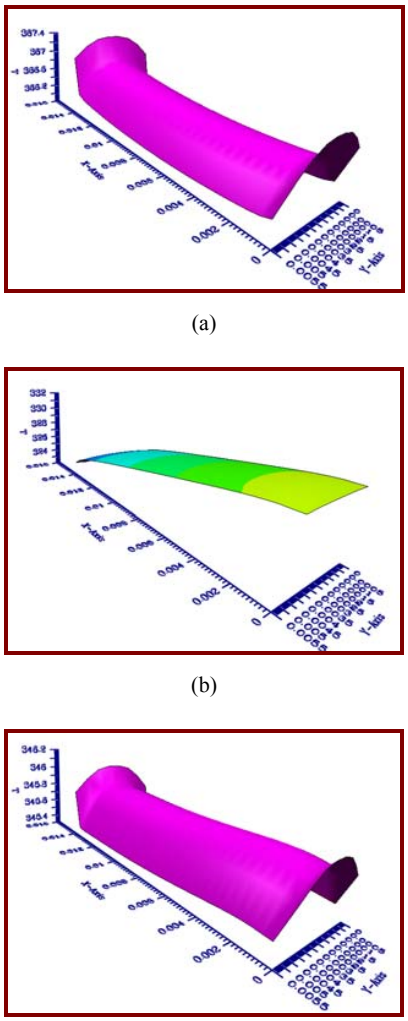

(a)

(b)

(c)

Fig. 6 The estimated temperature distributions over the PCR chip on the cross section at the depth of 1 mm below the chip surface at (a) 11 s (denaturation), (b) 25 s (annealing), and (c) 40 s (extension)

In order to perform a comprehensive analysis of the heat transfer mechanism in the chip, the cross-sectional temperature distributions are utilized to demonstrate the thermal characteristics inside the chip. A PDMS-glass bonding structure is selected to be the chip substrate in our designed chip. The thicknesses of the PDMS and glass substrates of the PDMS-glass bonding chip are 1 mm and 1 mm. The simulation results of the temperature distributions at the X-cut cross section at half the chip's length are shown in Fig. 7. The temperature spacing between the contour lines is 1 K. For a PDMS-glass bonding chip, the thermal conductivity of glass is much higher than that of PDMS and heat transfer occurs more efficiently cross the lower glass substrate, which reduces the temperature variation along the Z direction. The thin micro-device yields a lower thermal capacitance and a

reduction of the thermal resistance in the vertical direction, which decreases the temperature gradient in the Z direction. This makes the temperature distribution in the microchambers close to that of the aluminum block under the chip. From Fig. 7 it also can be found that the surface temperatures are lower than those at the chambers inside the chip, and the temperature differences between the chip surface and the PCR mixture are different at different measured points. During the PCR experiments the surface temperatures are usually measured to ensure that the chip setting temperatures are reached. The required PCR temperatures can be obtained by measuring the surface temperature of the chip and then adding the temperature difference between the chip surface and the PCR mixture. So the accuracy of the required PCR temperatures is dependent on the locations of the measured points.

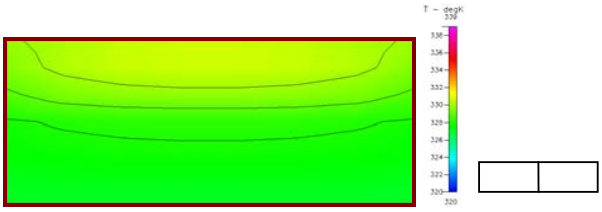

Fig. 7 The temperature distributions at the X-cut cross section at half the chip's length

To ensure the thermal requirement at three temperature steps of the PCR chip, the chip material should be chosen first. Because different materials have quite different thermal properties, which affect temperature distribution between different temperature steps, chip materials is surely the most important factor to be considered in chip design. The influences of various chip materials on the heat transfer are demonstrated in Fig. 8. PMMA, PDMS and PDMS-glass bonding structures are selected to be the chips' substrates. The thicknesses of the PMMA chip and the PDMS chip are both 2 mm. We assume the thicknesses of two substrates of the PMMA-PMMA and PDMS-PDMS bonding chips are 1 mm and 1 mm, respectively. The thicknesses of PDMS and glass substrates of the PDMS-glass bonding chip are 1 mm and 1 mm. The thermal conductivities of PMMA, PDMS and glass are 0.18, 0.15 and 0.78 W/mK, respectively. The simulation results of the temperature profiles along the central line (X direction) of the cross section at the depth of 1 mm below the chip surface are shown. The thermal conductivities of PMMA and PDMS are nearly the same, and thus the temperature difference between the PMMA chip and the PDMS chip is about 1 K. It shows very little difference. For a PDMS-glass bonding chip, the thermal conductivity of glass is much higher than that of PDMS and heat transfer occurs more efficiently across the lower glass substrate, which reduces the temperature variation along the z-direction. The temperature difference of the PDMS-glass bonding chip between the surface and the heater is lower than those of the PMMA and PDMS chips. So the temperature profiles of the PDMS-glass bonding chip are the highest among these three different chip materials during the denaturation and extension steps. And those are the lowest during the annealing step. For the PMMA and PDMS chips, the temperature of the chamber is less than the required temperature for denaturation and extension. Besides, the chamber's temperature is larger than the required annealing temperature.

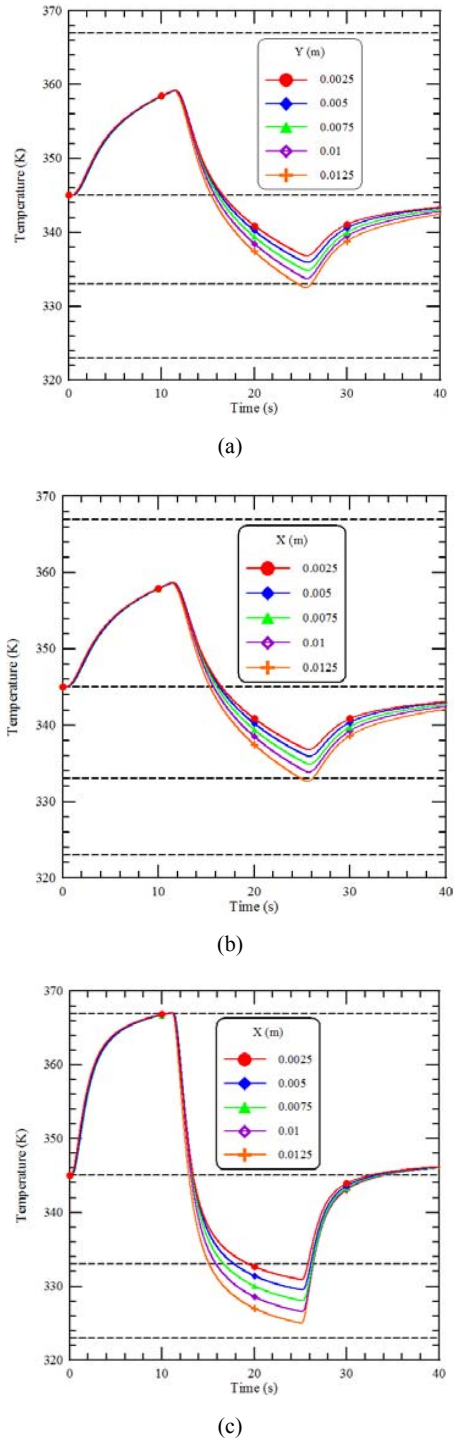


Fig. 8 The temperature distributions at the X-cut cross section at half the chip's length

With the purpose of improving the PCR yield, optimizing the annealing temperature would be preferred. By employing an aluminum block under the chip, the linear annealing temperature profile can be created. The influences of various thicknesses of the aluminum block on the temperature profiles along the central line of the cross section at the depth of 1 mm below the chip surface are shown in Fig. 9. For no aluminum block is used in Fig. 9(a), only conduction through the glass substrate can transfer the heat from the heater to the chip. It keeps the chip at a low temperature at the denaturation and extension steps and a high temperature at the annealing step. It reduces the heat transfer effect. The aluminum block with the thickness of 1 mm is utilized in Fig. 9(b). All three temperature steps have sufficient heating durations to perform PCR process. Compared to the results shown in Fig. 8(c) (the thickness of the aluminum block is 10 mm), the trend of the temperature profiles shows a very close similarity. However, the temperature uniformity at the denaturation and extension steps and the linearity at the annealing steps of the case of 10 mm thickness are better than that of the case of 1 mm thickness.

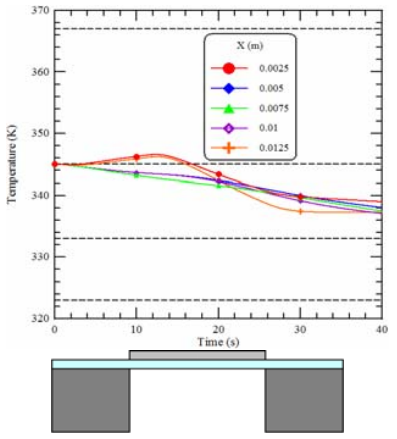


(a)

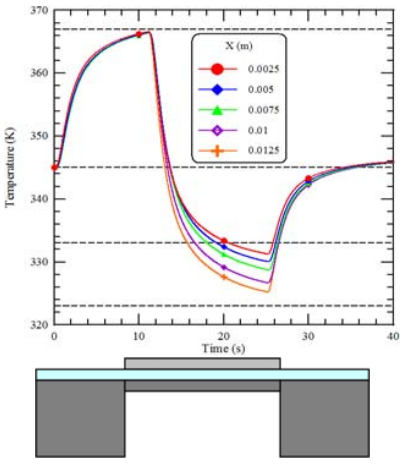


(b)

Fig. 9 The temperature distributions at the X-cut cross section at half the chip's length

In the PCR chip, three stable temperature zones compose its working zone. Large working zones are necessary to allow enough space for temperature cycling. That is to say to obtain high temperature uniformity on the chip at the denaturation and extension steps and high linear temperature profile on the chip at the annealing step is important. The influences of various thicknesses of the aluminum block under the chip on the cross-sectional temperature distributions at the denaturation, annealing, and extension steps are, respectively, illustrated in Fig. 10(a), 10(b), and 10(c). The thermal energy from the heater can be transferred through the aluminum block and then into the interior region of the chip. As the thermal conductivity of the material under the PDMS-glass bonding chip becomes large, the non-uniformity of the temperature distribution is small. The thermal conductivity of aluminum material is large, and the heat conduction for the aluminum block with larger thickness is greater than that with smaller thickness. The uniform temperature distribution can be clearly observed. Apparently, the design offers better uniformity in the chip with 10 mm thickness of the aluminum block compared that with 1 mm, as shown in Fig. 10(a) and 10(c). As expressed in Fig. 10(b), the temperature spacing between the contour lines is 1 K. We can find that the contour lines of the case with 1 mm thickness are shifted to the right compared to the case with 10 mm thickness. It means that the linearity of the temperature profile for the case with 10 mm thickness is better than that with 1 mm thickness.

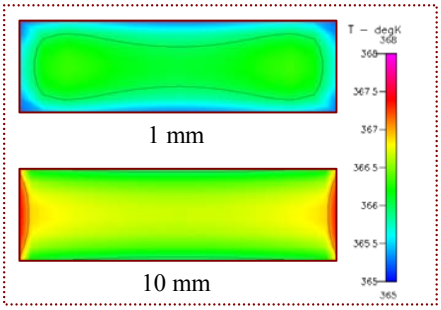


(a)

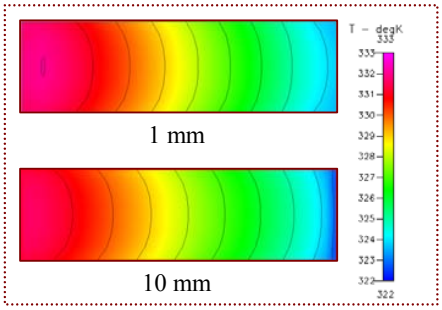


(b)

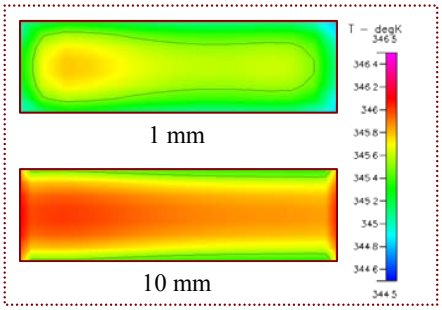


(c)

Fig. 10 The temperature distributions at the cross section at the depth of 1 mm below the chip surface for three temperature steps

Among PCR amplifications, the annealing temperature should be optimized to reach an effective and specific DNA amplification. The effect of various setting temperatures of two heaters at the annealing step on the temperature profiles along the central line on the cross section at the depth of 1 mm below the chip surface is depicted in Fig. 11. 5 different sets of the annealing temperature ranges are used to express the linearity of the thermal characteristics. Results show that a linear temperature profile can be found for each annealing temperature range.

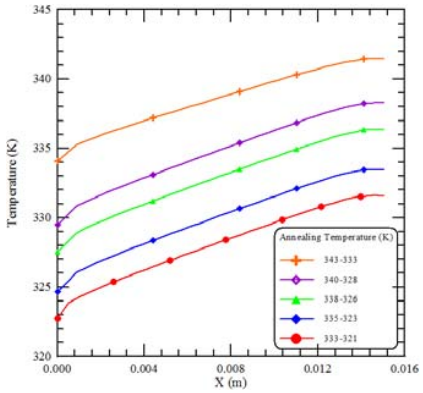


Fig. 11 The simulation results of the temperature profiles along the central line on the cross section at the depth of 1 mm below the chip surface

The stability of the PCR chip is examined and shown in Fig. 12. The thermal cycling profiles detected by the thermocouple inside the chamber for 10 cycles at 3 different locations are expressed. There shows no difference between the temperature profile of each cycle. Then the stability of the OSTRYCH is verified. Fig. 12 also shows experimental results of the temperatures at three different locations. Because of the high thermal conductivity of the aluminum block, the thermal interaction between two aluminum heating blocks is severe. The temperature difference of two heating blocks is not large, and then the linear temperature profile during the annealing step can not be obtained.

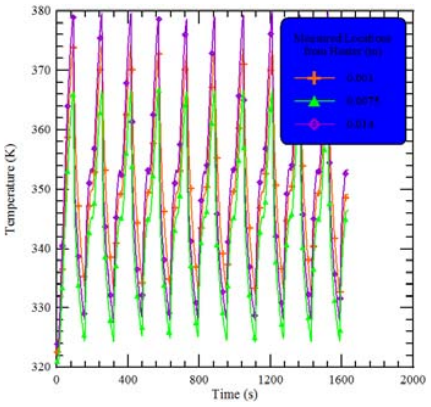


Fig. 12 The measured temperature profiles along the central line on the surface at three specific points

In order to improve the PCR yield, a uniform temperature distribution is one of the most critical factors in PCR amplification. An infrared camera is used to measure the surface temperature distribution in the PCR device. The IR images and the temperature distributions for three PCR steps are shown in Fig. 13. The uniform temperature distributions are observed between two temperature heaters at the denaturation and extension steps. It shows that the aluminum block under the chip is effective in generating the uniform temperature zone at the central part of the PCR chip. The temperature uniformity meets the temperature requirement of PCR amplification. In Fig. 13(b), the temperatures ranged from 52.8 °C (326 K) to 59.8 °C (333 K) at the annealing step can be illustrated. Due to the contact resistance between the chip and the aluminum block and the uncertain convective heat transfer coefficient outside the device, the linearity of the temperature is not well and the range of the annealing temperatures is needed to be improved. However, the comparison between the experimental data and numerical results shows a similar trend.

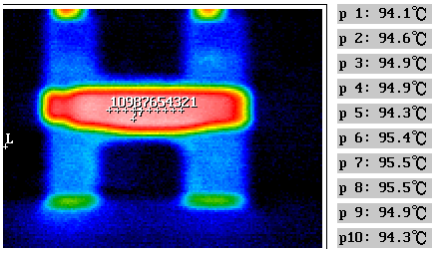


(a)

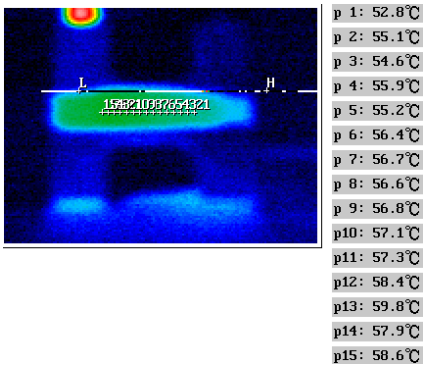


(b)

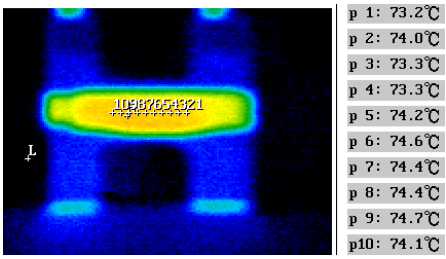


(c)

Fig. 13 IR imaging-based temperature distributions on the surface of the PCR chip at the (a) denaturation, (b) annealing, and (c) extension steps

## V. Conclusion

In this article, a novel linear temperature gradient concept used in the PCR device is tested. A PDMS-glass bonding chip is utilized to fabricate the device that provides up to five sample chambers. The numerical result shows that the center temperature of the chamber can achieve the reaction temperature during the reaction process. The influences of various chip materials on the heat transfer are examined, and the results show that the PDMS-glass bonding chip is the best choice. All three temperature steps have sufficient heating duration to perform PCR. The developed system is capable of performing parallel DNA amplifications with different annealing temperatures ranging from 326 K to 333 K.

## Acknowledgment

The authors would like to thank the National Science Council of the Republic of China for financially supporting this research under Contract No. NSC 101-2313-B-020-023-.

## References

[1] R. K. Saiki, S. Scharf, F. Faloona, K.B. Mullis, G. T. Horn, H. A. Erlich, and N. Arnheim, "Enzymatic amplification of beta-globin genomic sequences and restriction site analysis for diagnosis of sickle cell anemia," *Science*, vol. 230, pp. 1950–1954, 1985.

[2] M. A. Northrup, M. T. Ching, R. M. White, and R. T. Wltson, "DNA amplification in a microfabricated reaction chamber," in *Proceeding of the 7th international conference of solid state sensors and actuators*, pp 924–926, 1993.

[3] Q. Xiang, B. Xu, R. Fu, and D. Li, "Real time PCR on disposable PDMS chip with a miniaturized thermal cycler," *Biomed. Microdevices*, vol. 7, pp. 273–279, 2005.

[4] T. Ohashi, H. Kuyama, N. Hanafusa, and Y. Togawa, "A simple device using magnetic transportation for droplet-based PCR," *Biomed. Microdevices*, vol. 9, pp. 695–702, 2007.

[5] Y. Sun, N. T. Nguyen, and Y. C. Kwok, "High-throughput polymerase chain reaction in parallel circular loops using magnetic actuation," Anal. Chem., vol. 80, pp. 6127–6130, 2008.

[6] N. Ramalingam, Z. Rui, H. B. Liu, C. C. Dai, R. Kaushik, B. Ratnaharika, and H. Q. Gong, "Real-time PCR-based microfluidic array chip for simultaneous detection of multiple waterborne pathogens," *Sensor. Actuat. B-Chem.*, vol. 145, pp. 543–552, 2010.

[7] C. Zhang, and D. Xing, "Microfluidic gradient PCR (MG-PCR): a new method for microfluidic DNA amplification," *Biomed. Microdevices*, vol. 12, pp. 1–12, 2010.

[8] E. Wulff-Burchfield, W. A. Schell, A. E. Eckhardt, M. G. Pollack, Z. Hua, J. L. Rouse, V. K. Pamula, V. Srinivasan, J. L. Benton, B. D. Alexander, D. A. Wilfret, M. Kraft, C. B. Cairns, J. R. Perfect, and T. G. Mitchell, "Microfluidic platform versus conventional real-time polymerase chain reaction for the detection of *Mycoplasma pneumoniae* in respiratory specimens," *Diag. Micr. Infec. Dis.*, vol. 67, pp. 22–29, 2010.

[9] D. Sugumar, L. X. Kong, A. Ismail, M. Ravichandran, and L. S. Yin, "Rapid multi sample DNA amplification using rotary-linear polymerase chain reaction device (PCRDisc)," *Biomicrofluidics*, vol. 6, 014119, 2012.

[10] D. Liu, G. Liang, X. Lei, B. Chen, W. Wang, and X. Zhou, "Highly efficient capillary polymerase chain reaction using an oscillation droplet microreactor," *Anal. Chim. Acta*, vol. 718, pp. 58–63, 2012.

[11] J. P. Holman, *Heat Transfer*, 10th ed. McGraw-Hill, New York, 2009.

[12] T. J. Barth, and D. C. Jespersen, "The design and application of upwind schemes on unstructured meshes," in *27th Aerospace Sciences Meeting and Exhibit*, AIAA-89-0366, 1989.

[13] L. H. Howell, R. B. Pember, P. Colella, J. P. Jessee, and W. A. Fiveland, "A conservative adaptive-mesh algorithm for unsteady, combined-mode heat transfer using the discrete ordinates method," *Numer. Heat Tr. B-Fund.*, vol. 35, pp. 407–430, 1999.

[14] J. J. Chen, C. H. Chen, and S. R. Shie, "Optimal designs of staggered Dean vortex micromixers," *Int. J. Mol. Sci.*, vol. 12, pp. 3500–3524, 2011.

**Sin J. Chen** received the B.S.E. degree in biomechatronics engineering from National Pingtung University of Science and Technology, Taiwan, in 2011. Currently, he is pursuing the M.S. degree in biomechatronics engineering from National Pingtung University of Science and Technology, Taiwan. His research interests lie Lab on a chip technologies, and thermal control module.

**Jyh J. Chen** received the PhD degree in mechanical engineering from National Chiao Tung University, Taiwan, in 1999, respectively. Since autumn 2010, he worked as an associate professor at National Pingtung University of Science and Technology, Taiwan. His research interests are microfluidics, and BioMEMS as well as computational simulation.